

# Theoretical and Experimental Aspects of Carbon Formation in Thermal Plasma

K. A. Főglein<sup>1</sup>, J. Gubicza<sup>3</sup>, I. Z. Babiewskaya<sup>4</sup>, J. Szépvölgyi<sup>1,2</sup>

<sup>1</sup>*Institute of Materials and Environmental Chemistry*

*Chemical Research Center, Hungarian Academy of Sciences, Budapest, Hungary*

<sup>2</sup>*Research Institute of Chemical and Process Engineering, University of Pannonia, Veszprém, Hungary*

<sup>3</sup>*Department of Solid State Physics, Eötvös University, Budapest, Hungary*

<sup>4</sup>*Institute of General and Inorganic Chemistry, Russian Academy of Sciences, Moscow, Russia*

## Abstract

Formation of carbon black from Freons was studied in RF thermal plasma conditions. Equilibrium compositions of the products were calculated by computer code ASTRA 4.0. The experiments on thermal decomposition were performed in an RF thermal plasma reactor. By comparing the calculated and experimental results a model was constructed on carbon black formation in RF thermal plasma reactor.

**Keywords:** Freons, carbon black, RF thermal plasma, modeling

## 1. Introduction

Decomposition of chlorine and fluorine containing hydrocarbons (Freons) is in the focus of research for quite a time. It is reasoned by the ozone depletion capability of particular compounds on one hand, and their strong greenhouse effects on the other. Catalytic methods [1] and plasma processing [2] seem to be suitable technologies for the decomposition of halogenated methane derivatives.

It has been established that decomposition of particular compounds in neutral or reactive atmosphere led to formation of different solid carbon species [3-5]. These findings may open new vistas in the processing of Freons. However, mechanism and kinetics of carbon formation during thermal decomposition is poorly understood yet.

In thermal plasmas the materials are treated in special circumstances such as very high temperature, intensive heat and mass transfer, very rapid cooling of reaction products and local equilibrium conditions. Thus, Freons can be completely decomposed in thermal plasmas along with the production of soot and carbon black (CB). In this paper results of thermodynamic calculations and experiments on the decomposition of three Freons ( $\text{CCl}_4$ ,  $\text{CHCl}_3$  and  $\text{CFCl}_3$ ) are discussed.

## 2. Thermodynamic calculations

In order to get information on the equilibrium compositions during decomposition of Freons in thermal plasmas we performed thermodynamic calculations in the temperature range of 298 - 6000 K by computer code ASTRA 4.0 based on the minimization of Gibbs free enthalpy.

It is known that in thermal plasma decompositions the first condensed material that appears on cooling of gaseous species will be the main reaction product.

In the calculations we assumed that even solid carbon participates in the equilibrium. According to our calculations, in order to get solid carbon as main reaction product the temperature of gaseous species should be decreased with a high rate from 1000 to 298 K (Fig. 1).

The carbon yields in equilibrium conditions are changing in the following order:

$\text{CFCl}_3 < \text{CCl}_4 \approx \text{CHCl}_3$  at 1000 K and

$\text{CFCl}_3 \approx \text{CCl}_4 < \text{CHCl}_3$  at 298 K.

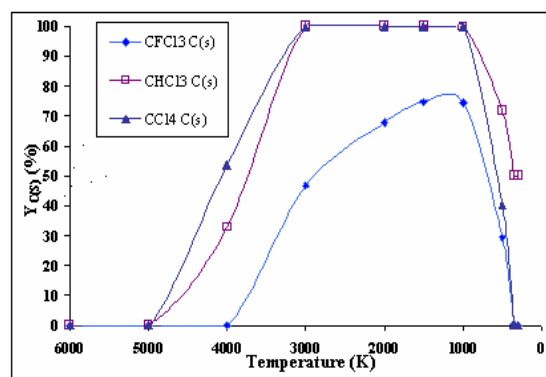


Fig. 1 Thermodynamic calculations on the solid carbon yields in argon atmosphere

In order to have a deeper insight into decomposition processes we performed thermodynamic calculations by taking into consideration the gaseous carbon radicals such as C,  $\text{C}_2$ ,  $\text{C}_3$ ,  $\text{C}_4$  and  $\text{C}_5$ , as well. The calculations (Fig. 2) show that gaseous carbon radicals formed from  $\text{CFCl}_3$  are preserved at much lower temperatures than the same radicals from other precursors. Below 4000 K concentration of gaseous carbon originated from  $\text{CFCl}_3$ , is much higher compared to the other ones which leads to formation of higher amount of soot and hence, formation of more CB in the  $\text{CFCl}_3$  case.

## 3. Experimental

The experiments were carried out in an RF thermal plasma reactor made of quartz glass. The RF generator operated at 27 MHz with plate powers of 1-4 kW [6].

All model compounds ( $\text{CCl}_4$ ,  $\text{CHCl}_3$  and  $\text{CFCl}_3$ ) were Aldrich products. Gases from Linde Co were used as cen-

tral, sheath and carries gases, respectively. The initial gas compositions are listed in Table 1.

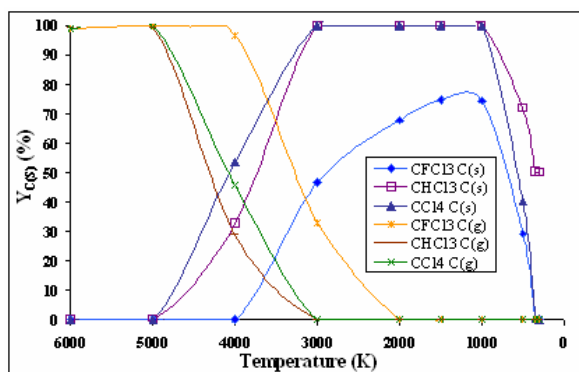


Fig. 2 Thermodynamic calculations on the yields of solid carbon and gaseous species, respectively in argon atmosphere

Table 1 Initial gas compositions

System	Precursor	Gas composition (m%)		
		Precursor	Ar	H <sub>2</sub>
1	CCl <sub>4</sub>	0.93	99.07	-
2	CHCl <sub>3</sub>	1.15	98.85	-
3	CFCl <sub>3</sub>	1.15	98.85	-
4	CFCl <sub>3</sub>	3.52	96.45	0.03

The main reaction product was solid soot which mostly condensed on the air-cooled reactor wall. Further amounts of soot portions were separated in two collectors attached to the plasma reactor [6]. The solid soot contained different adsorbed hydrocarbons. To separate them and to get CB (C(s)) as main product, the soot was extracted by toluene. The CB yield ( $Y_{C(s)}$ ) was calculated as follows:

$$Y_{C(s)} = \frac{\text{Rate of carbon black formation (mol}\cdot\text{h}^{-1})}{\text{Feed rate of precursor (mol carbon}\cdot\text{h}^{-1})} \quad (1)$$

The soot and CB samples were investigated by X-ray diffraction (XRD) in a Philips X'pert powder diffractometer using a CuK<sub>α</sub> radiation ( $\lambda=0.15418$  nm) and a pyrolytic graphite secondary monochromator.

#### 4. Experimental design by STATISTICA code

To get detailed information on the change of  $Y_{C(s)}$  against process conditions, the thermal plasma experiments were designed by STATISTICA code. In the experimental design factors and levels should be determined. The factors are parameters that change independently of each other during the experiments, while the levels are the values of factors. In our work composition and feed rate of Freons and the plate power of RF generator were selected as factors. Each factor had three levels. The software generated a 3×3 Greco-Latin Square (Table 2). Thus, nine experiments should be performed to have as much information as possible on the effects of factors on  $Y_{C(s)}$ .

Table 2 The Greco-Latin Square for Systems 1-3

Run No.	Precursor	Plate power (kW)	Feed rate (mol·h <sup>-1</sup> )	$Y_{C(s)}$
1	CCl <sub>4</sub>	1.6	0.15	10.8
2	CCl <sub>4</sub>	2.1	0.30	15.7
3	CCl <sub>4</sub>	2.6	0.45	29.7
4	CHCl <sub>3</sub>	1.6	0.30	35.6
5	CHCl <sub>3</sub>	2.1	0.45	36.2
6	CHCl <sub>3</sub>	2.6	0.15	34.3
7	CFCl <sub>3</sub>	1.6	0.45	43.7
8	CFCl <sub>3</sub>	2.1	0.15	28.7
9	CFCl <sub>3</sub>	2.6	0.30	36.6

From the plotting of experimental results (Fig. 2) we can establish that

- the carbon black yield depends on composition of precursors,
- the  $Y_{C(s)}$  values are changing in the following order: CCl<sub>4</sub> < CHCl<sub>3</sub> < CFCl<sub>3</sub>,
- the plate power has a complex effect on  $Y_{C(s)}$  and
- increase of feed rate leads to higher  $Y_{C(s)}$  values.

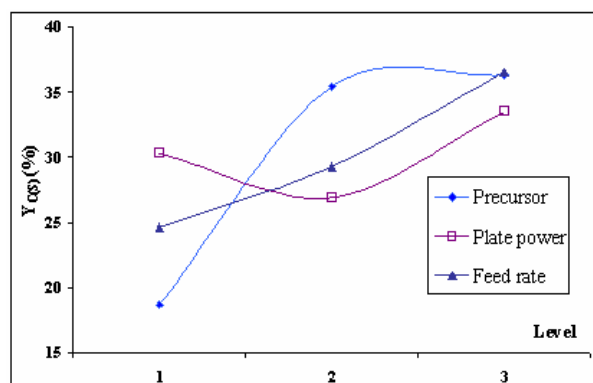


Fig. 3 CB yield as plotted against the levels of different factors

The experimental results relating to the effect of precursor composition on  $Y_{C(s)}$  were differing from those of thermodynamic calculations. In equilibrium conditions, the lowest  $Y_{C(s)}$  was obtained for CFCl<sub>3</sub>, while in the experiments the highest yields were detected exactly in this case. The reasons will be discussed below.

The mean plasma temperature and the mean residence time of reagents are increased with the plate power. It results in higher ionization and thus, more effective decomposition of precursors. However, the chance of secondary reactions leading to undesirable products also increases. Decomposition of Freons to carbon and reactions of primary products are competitive processes which make the overall picture much more complicated.

Even the feed rate of Freons has an effect on  $Y_{C(s)}$ . The higher the feed rate the higher the carbon concentration in the hot zone which leads to higher CB yields.

## 5. Results and discussion

Comparison of experimental data (Table 2) with the results of thermodynamic calculations (Fig. 1) reveals that

- all experimental  $Y_{C(S)}$  values are lower than the equilibrium yields calculated at 1000 K.
- In case of  $CFCl_3$  and  $CCl_4$  higher  $Y_{C(S)}$  values were obtained in the experiments as compared to the equilibrium ones at 298 K.
- Order of precursors in terms of  $Y_{C(S)}$  are different in the equilibrium and actual cases, respectively; the experimental  $Y_{C(S)}$  values increase in the following order:  $CCl_4 < CHCl_3 \approx CFCl_3$ , while in thermodynamic equilibrium the relevant order is  $CFCl_3 < CCl_4 \approx CHCl_3$  at 1000 K and  $CFCl_3 \approx CCl_4 < CHCl_3$  at 298 K.

The first finding as above refers to non-equilibrium conditions during the decomposition of given precursors in particular conditions. The precursors completely decomposed to smaller fragments. However, these intermediates had a short residence time in the hot zone. They cool down very rapidly and thus, may exist even at low temperatures.

To investigate the degree of CB crystallization against process conditions in the case of  $CFCl_3$ -Ar- $H_2$  system (Table 1, System 4) XRD measurements were carried out on soot and CB samples from different sections of the experimental set-up. From the diffractograms (Figs. 4 and 5), we determined the integrated area, the width and the height of peaks at  $2\Theta$  values of 20.20, 29.36 and 39.56 degrees, respectively (Table 3). The crystallite size was calculated as follows:

$$D = \frac{0.9 \cdot \lambda}{\cos \Theta \cdot \Delta(2\Theta)} \quad (2)$$

where  $D$  (nm) is the grain size of crystallites,  $\lambda$  (nm) is the wavelength of X-rays used for the measurements and  $\Theta$  (rad) is the diffraction angle of the first strong X-ray peak. The nearest neighbor distance was calculated as follows:

$$a = \frac{0.9 \cdot \lambda}{2 \cdot \sin \Theta} \quad (3)$$

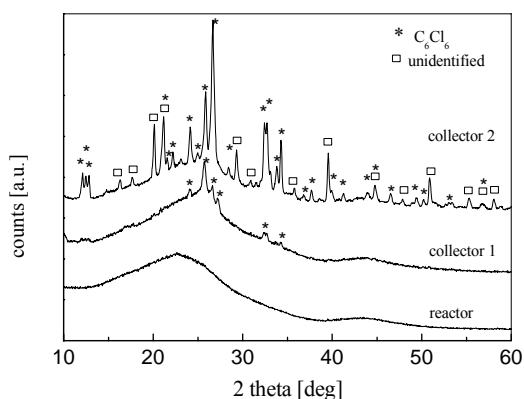


Fig. 4 X-ray diffractograms of different soot samples

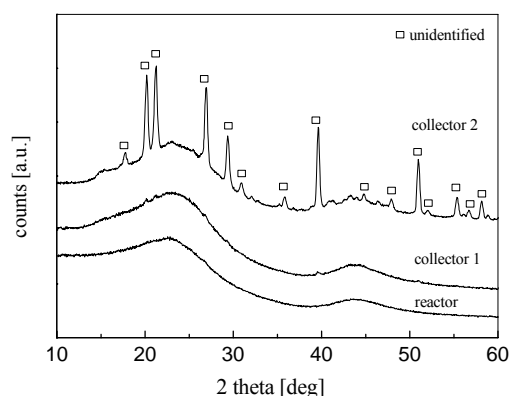


Fig. 5 X-ray diffractograms of different carbon black samples

From the XRD investigations (Figs 4-5 and Table 3) the following conclusions can be drawn:

- soot collected in the reactor is amorphous, while products separated in collectors 1 and 2 are mainly crystalline materials; the main crystalline phases are hexachloro-benzene and an up-to-now unidentified material.
- The crystalline fraction in C(S) increases with the distance from the plasma flame (reactor  $\rightarrow$  collector 1  $\rightarrow$  collector 2). The integrated area ratio of soot and CB samples normalized by their mass is about 0.5 (Table 3 (a)) which means that CB is more crystalline than the soot.
- The grain size ratio of the soot and CB is 1.5 (Table 3 (b)) indicating greater primary grains in the soot.
- The centre of the amorphous band shifted from  $2\Theta$  degree of 22.6 to higher values against the distance from the plasma flame (Table 3 (c)). The nearest neighbor distance calculated from the position of the centre of amorphous band decreased against the distance from plasma flame (Table 3 (d)), as well.

Based on above findings we constructed a model on carbon black formation in RF thermal plasma conditions. The soot particles have an inner core consisting of both amorphous and crystallized carbon, covered by a surface layer of organic compounds (such as  $C_6Cl_6$ ). The mean crystal size of soot is 33.6 nm (Table 3 (b)). During toluene extraction the surface layer is removed along with some portion of the bulk as it is justified by the decrease of mean grain size from 33.6 to 22.4 nm (Table 3 (b)).

The higher the distance from the plasma flame, the closer are the carbon atoms in the amorphous fractions. It results in a shifting of the amorphous hump in X-ray diffractogram (Table 3 (c)) to higher  $2\Theta$  values indicating the decrease of the nearest neighbor distance (Table 3 (d)). At greater distances from the plasma flame products being more crystallized even in the inner core were separated. We explain it by the longer condensation time of particular species as compared to particles condensed

immediately on the air-cooled reactor wall. The CB content of the soot also depends on the distance from the plasma flame: the higher the distance the lower the CB content of the soot (Table 3 (e)).

### Conclusions

Effects of processing conditions on carbon black yield were determined during decomposition of  $\text{CCl}_4$ ,  $\text{CHCl}_3$  and  $\text{CFC}_3$  in RF thermal plasma reactor. It was found that the CB yield mainly depended on the composition of

Freons. The feed rate and the plate power affected the CB yield in less extent.

XRD investigations of the soot and the CB revealed that the soot particles have an inner core consisting of amorphous and crystallized carbon which is covered by a surface layer of chlorine-containing organic molecules. Ratio of the surface layer and the inner core changes against the thermal history of materials i.e. against the distance of sampling from the plasma flame.

Table 3 Results of XRD investigations for System 4

Peak angle ( $2\Theta$ degree)	XRD results		Distance from the top of plasma flame (cm)	XRD results		e
	a	b		c	d	
20.20	0.482	33.6/22.4=1.5	47.5 (reactor)	22.6	0.354	82.57
29.36	0.482		82.5 (collector 1)	22.9	0.350	68.00
39.56	0.508		123.2 (collector 2)	23.0	0.348	55.36
Mean	0.491	33.6/22.4=1.5				

a Integrated area ratios of the soot and C(S) samples normalized by their mass

b Grain size ratio of the soot and C(S) sample (D/nm)

c Angle of the center of the amorphous X-ray peak depending on the distance from the plasma flame ( $2\Theta$ )

d Nearest neighbor distance depending on the distance from the plasma flame (a/nm)

e CB content of the soot (m/m%; mass ratio of CB and soot, after and before the extraction)

### Acknowledgement

This work has been supported by Hungarian Scientific Research Fund (OTKA) Grant Nos. F047057 and T047360.

### References

- [1] Y. Takita, J. Moriyama, Y. Yoshinaga, H. Nishiguchi, T. Ishihara, S. Yasuda, *Applied Catalysis A-General* **271(1-2)**, 55 (2004).
- [2] K. A. Főglein, P. T. Szabó, I. Z. Babievskaya, J. Szépvölgyi, *Plasma Chemistry and Plasma Processing* **25(3)**, 289 (2005).
- [3] L. B. Avdeeva, T. V. Reshetenko, V. B. Fenelonov, A. L. Chuvilin, Z. R. Ismagilov, *Carbon* **42(12-13)**, 2501 (2004).
- [4] J. J. Wang, M. Y. Zhu, R. A. Outlaw, X. Zhao, D. M. Manos, B. C. Holloway, *Carbon* **42(14)**, 2867 (2004).
- [5] U. Narkiewicz, W. Arabczyk, W. Konicki, *Fullerenes Nanotubes and Carbon Nanostructures* **13 Suppl. 1**, 99 (2005).
- [6] K. A. Főglein, J. Szépvölgyi, P. T. Szabó, E. Mészáros, E. Pekker-Jakab, I. Z. Babievskaya, *Plasma Chemistry and Plasma Processing* **25(3)**, 275 (2005).